AIRCRAFT FUEL TANK INSPECTION WITH HEXAPOD MOBILE ROBOT

Adrian Olaru[1], Maria-Giorgiana Khan Gaina[2]
[1] Prof.Ph.D.eng. "POLITEHNICA" University of Bucharest, Romania
[2]Ph.D.stud.eng. "POLITEHNICA" University of Bucharest, Romania
Emails: aolaru_51@ymail.com, mariagiorgiana_gaina@yahoo.com

Abstract - A large number of inspections and modifications of the aircraft's fuel tanks as well as their adjacent systems must be made inside them. The necessary maintenance and repair tasks must be performed by technical personnel, who must physically enter the fuel tank, where it is exposed to many environmental risks. These potential risks include: fire and explosion, toxic and irritating chemicals, oxygen deficiency, and the limited nature of the fuel tank. This paper focuses on modeling and simulating the movement of the hexapod mobile robot using LabView 14.04 used in the interior of the aircraft fuel tank inspecton. The analysis will help to demonstrate if the mobile robot is fit for this such activities and protect the human factor.

Keywords: Modeling, Simulating, Control, Inspection, Aircraft fuel tank, Hexapod Mobile robot.

1. Introduction

Entry into airplane fuel tank is needed for inspections and modifications, but these works may pose a risk factor for technical staff (fig. 1). Working in the fuel tank can be done safely if technical staff is trained especially has the necessary equipment. In this area robots can intervene successfully.

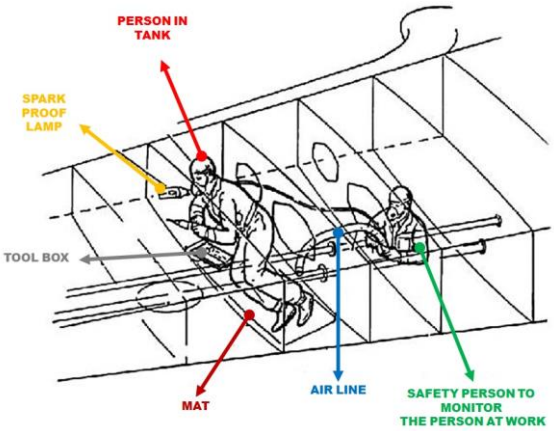

Figure 1: Technical staff entry into aircraft fuel tank

Therefore, this paper aims to implement a mobile robot. Due to its characteristics, the robot can easily sneak into the fuel tank of the aircraft and the operator can guide robot from outside to facilitate its aircraft maintenance activities.

The main problem of an autonomous mobile robot is to carry out the control of locomotion on land.

Some of the structures used to build mobile robots have been obtained thanks to the inspiration of the animal kingdom, such as the hexapod. Several researchers were inspired and then relied on, emulating the four-legged animals or insects.

Among the most remarkable legged robots we could mention the "Big-Dog" with four legs which is operating military applications, but also "RHex" (Moore, 2002) and "MELMANTIS" (Melmantis, 1997) [1-10].

A legged robot has the ability to move on land with a high degree of difficulty, which is why mobile wheeled robots do not have this advantage. Robots with legs can move over landslides, gravel, uneven roads, obstacles or land where there are no roads. However, the ability to control a hexapod robot is a complex issue.

The system of robot locomotion employed, coordinated simultaneous movement and consists of six legs, each with three degrees of freedom (DOF). The Hexapod robot (fig. 2) has 18 degrees of freedom [1-11, 12].

Due to the fact that the movement of the robot is achieved by interaction of unstructured environment, it is necessary to understand the specific use of an electronic system for obstacles detection.

However, it should be stressed that the main problem is the coordination of angular movement of the robot's 18 joints during movement, emphasizing the sequence of steps. This problem is achieved by implementing an electronic system dedicated to distributive architecture.

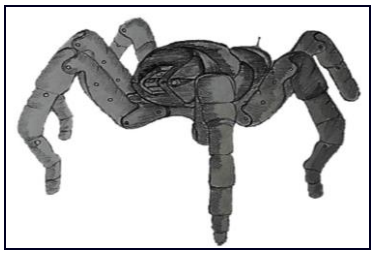

Figure 2: Hexapod mobile robot

2. Hazards in the Fuel Tank and Microbial Environment

The most common and recognized danger of the tank is the fuel itself. Fuel is a flammable liquid that can ignite under certain environmental conditions, temperature and vapor concentration. The temperature at which the vapors of a flammable liquid can "ignite" is known as the flash point. A hazardous concentration of vapor is present when a fuel vapor reaches a level known as the Lower Flammability Limit (LFL) or Lower Explosive Limit (LEL). These limits are usually expressed as a percentage of the volume. Fuels below LFL / LEL (Lower Flammability Limit / Lower Explosive Limit) are considered too weak to burn. If the fuel vapor concentration exceeds the upper flammability limit or the upper explosion limit, the fuel is considered too rich to burn. A concentration of fuel vapor between these two limits is considered to be in its flammable range, it will ignite and burn in contact with an ignition source. One of the best ways to control unwanted fires and explosions is to to keep the fuel vapor concentration below the LFL / LEL (Lower Flammability Limit / Lower Explosive Limit), thus preventing it from reaching its flammability range [13], [15].

Other flammable chemicals may also be present during maintenance and repair work in the fuel tank. Chemicals with a low flash point (less than 70 ° F (21 ° C)), such as methyl kenone (MEK), are more dangerous than fuel in the tank, so their use must also be be strictly controlled [13], [15].

Chemicals, including fuel, can also present a toxic or irritating hazard. In high concentrations, the fuel together with other hydrocarbons can affect the nervous system, causing headaches, dizziness and lack of coordination. Chemicals can cause chronic health problems, which can affect the liver and kidneys, skin irritations if left unchecked.

An aircraft maintenance mechanic is exposed to an inhalation of kerosene : 1 – 15 mg/m^3 and in the realistic worse case will be : 420 mg.d^{-1} on an surface of 420 cm^2 [16]. The most common health problems due to kerosene are chemical pneumonitis and vomiting, due to the inhalation of the vapors in the aircraft fuel tank. In some cases, if the technical staff is more sensitive, inhalation of kerosene vapor can lead to heart attack and over a longer period of time it may even be predisposed to cancer.

The aircraft fuel tank is also inspected for contaminants such as water or microbial growth, sediment etc. A common and serious potential contaminant of the fuel is water. Water can accumulate and contaminate the fuel of the aircraft at any depot or refueling the aircraft fuel tank. An accumulation of water within a fuel tank can provide an atmosphere for microbial growth. Microbial growth produces a variaty of chemicals that are harmful to fuel systems including: hydrogen sulfide, protein coating, organic acids etc. Microbial growth as a brownish silty substance with a gelatinous consistency, called “Apple Jelly” [17-20]. Microbial growth can cover the components of the fuel systems and can eventually cause clogging of filters of the engines and pipes, causing deficiencies in the fuel system or anomalies and deterioration of the protective layer which can lead to corrosion [17-20].

To prevent all the negative effects, drain the aircraft fuel tank frequently. Use the specified fuel drain probes and use available test items to detect signs of microbial growth. If large quantities of jelly are present in only one of the tank, a thorough inspection of the fuel must be carried out on the rest of the aircraft fuel tanks.

Good hygiene fuels involves the implementation of a “rigid cleaning regime” assessed for risk. The risk of contamination is increased in hot and humid conditions, especially when the fuel comes from a source that has fewer quality control controls.

An aircraft which have no history of microbiological contamination, can be considered – low risk, this being the ideal scenario. Unfortunately, there are other aircrafts that show the possible appearance of bacteria. For increased aicraft safety the test should be performed regardless of the scenario. For performing the aircraft fuel test, I preferred to show the test with MICROBMONITOR2 [21], described below:

Step 1 –With the help of an syringe add 0,5 ml fuel to the Microbmonitor2 bottle. Close the bottleand put a label

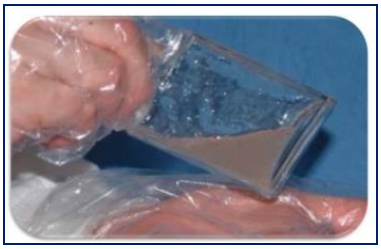

Step 2 –Tap the bottle until you see the gel

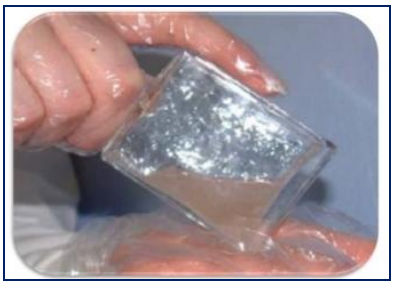

Step 3 – Sake the bottle for 30 s

Step 4 –Try to put the gel into the bottom of the bottle

Step 5 –Try to make a flat layer of gel and rest. Keep the bottle in a warm and a dark place at 25 °Cfor 4 days. (Can be examinated daily)

Step 6 – Examine the content of the bottle

Figure 3: Aircraft fuel test procedure with MICROBMONITOR2 [21]

For the human factor to use this proceduse is simple. The aircraft mechanic need to use gloves and avoid touching the inside of the bottle. After use the bottle, the aircraft mechanic need to wash the hands, because the bottle contain microbial growth. For the aircraft mechanic health, he must have a proper hygiene every time he use/touches the bottle. The battle with the microbial growth have not yet been shown to have a drastic negative on the human factor.

To interpret the test of the aicraft fuel are presented some IATA [20] compliant verification advice:

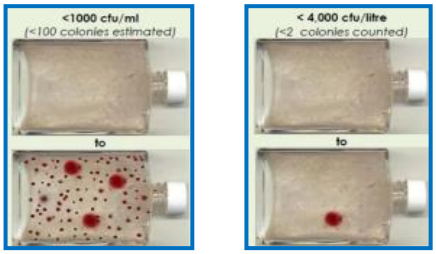

1-Water (if present) 2-Fuel

A) ACCEPTABLE

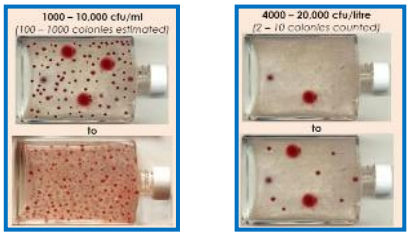

1-Water (if present) 2-Fuel

B) MODERATE

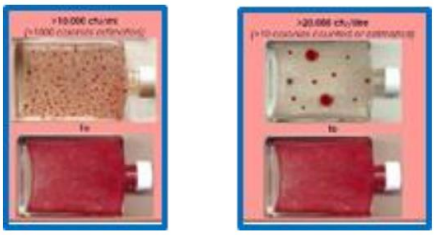

1-Wather (if present) 2-Fuel

C) NOT ACCEPLABLE

Figure 4: Interpretation of results [21]

Another method used in maintenance for microbiological contamination is the use of the - "fuelstat-resinae-plus-fuel-test-kit" (fig. 5). This method is more simple to use because you just have to put the fuel in the test and the result you will have in just 15 minutes.

Step 1 – Put the fuel in the test

Step 2 – After 15 min examine the result

Figure 5. Fuelstat resinae plus - fuel test kit [23]

Following this analysis of work in the aircraft's fuel tank, it appears that this working environment is very harmful to humans exposed for a long period of time. Therefore, the main purpose of this paper is to show this problem and to try as much as possible to reduce the negative effects on the human factor by introducing a mobile robot. The mobile robot can be a real help to the human factor in order to reduce the exposure time inside the aircraft's fuel tank.

3. Cinematic Model of a Foot

It is important to select a configuration mechanical robot leg that maximizes movement and requires a minor amount of restriction in its locomotion. For the implementation of each leg of the hexapod robot was used a driveline with three turns or RRR joint. Direct geometric model for each foot mechanism was formulated using a mobile frame $O_i(x_i, y_i, z_i)$ for each joint, with i=1..2 and a fixed frame $O_W(X_W, Y_W, Z_W)$ [11]. The various links of the robot legs have been named as: coxa, femur and tibia. The reference framework leg hexapod robot starts with zero touch, which is the structure of the robot, where the foot is anchored or mounted on the ground; one is coxa link, the link is two femur and tibia connection with three is the final end as the base. To calculate the direct of Kinematic equation is to use Denavit-Hartenberg parameters, change by Craig (Ollero, 2007) and has yielded the following matrix transformation [3-5]:

$$T_1^0 = \begin{bmatrix} cos(q_1) & -sin(q_1) & 0 & 0 \\ sin(q_1) & cos(q_1) & 0 & 0 \\ 0 & 0 & 1 & 0 \\ 0 & 0 & 0 & 1 \end{bmatrix}$$
$$T_2^1 = \begin{bmatrix} cos(q_2) & -sin(q_2) & 0 & l_1 \\ sin(q_1) & cos(q_2) & 0 & 0 \\ 0 & 0 & 1 & 0 \\ 0 & 0 & 0 & 1 \end{bmatrix} \quad (1)$$
$$T_{OT}^2 = \begin{bmatrix} 1 & 0 & 0 & l_2 \\ 0 & 1 & 0 & 0 \\ 0 & 0 & 1 & 0 \\ 0 & 0 & 0 & 1 \end{bmatrix}$$

where: q_1 is the angle of the femur [degrees]; q_2 is the angle of tibia [degrees]; l_1 is far femur [cm]; l_2 is far tibia [cm].

To find the matrix transformation T_{OT}^0 is the product of $T_1^0 \cdot T_2^1 \cdot T_{[OT]}^2$ [3, 4, 7]. The result corresponds to the following equations for direct kinematics for each leg of the hexapod robot, so the coordinates of the final end of a leg of the robot are:

$$x = l_1 cos(q_1) + l_2 cos(q_1 + q_2)$$
$$y = l_1 sin(q_1) + l_2 cos(q_1 + q_2) \quad (2)$$

While joint kinematics differential speeds with speeds relate directly to the desktop via the robot Jacobian matrix, this method is obtained by propagation velocity, whose equation are [1-10]:

$$v = \begin{bmatrix} 0 \\ 0 \\ \dot{q}_1 \end{bmatrix} \times \begin{bmatrix} x \\ y \\ 0 \end{bmatrix} + R_2^0 \left(\begin{bmatrix} 0 \\ 0 \\ \dot{q}_2 \end{bmatrix} \times \begin{bmatrix} l_2 \\ 0 \\ 0 \end{bmatrix} \right)$$
$$R_2^0 = \begin{bmatrix} cos(q_1 + q_2) & -sin(q_1 + q_2) & 0 \\ sin(q_1 + q_2) & cos(q_1 + q_2) & 0 \\ 0 & 0 & 1 \end{bmatrix} \quad (3)$$

V is the vector of the translation speed of the end of the tibia [cm/ s], $\dot{q}_1$ and $\dot{q}_2$ speed actuators [degrees/ and]. Expanding equation (3) can get a reduced Jacobian, which is:

$$J(q) = \begin{bmatrix} j_{11} & j_{12} \\ j_{21} & j_{22} \end{bmatrix}$$
$$j_{11} = -l_2 sin(2q_1 + 2q_2) + l_1 sin(q_1) + l_1 sin(2q_1 + q_2)$$
$$j_{12} = -l_2 sin(q_1 + q_2) \quad (4)$$
$$j_{21} = l_2 cos(2q_1 + 2q_2) + l_1 cos(q_1) + l_1 cos(2q_1 + q_2)$$
$$j_{22} = l_2 cos(q_1 + q_2)$$

Therefore, direct differential kinematics is defined as:

$$\begin{bmatrix} \dot{x} \\ \dot{y} \end{bmatrix} = J(q) \begin{bmatrix} \dot{q}_1 \\ \dot{q}_2 \end{bmatrix} \quad (5)$$

where $\dot{x}$ and $\dot{y}$ are translational velocities [cm/ s] of the distal tibia with the plan [11].

4. Inverse Cinematic

The geometric variables described above establishes the connection between the joints, the position and orientation of the frame located at the foot. The problem of inverse kinematic model is to determine variables joints, starting from a position and orientation of the frame located at the end. To solve this problem, we need to understand the importance of specific variables and joint motion trajectories for each leg of the hexapod robot [1-11]. These paths are obtained from the time the movement path is processed being attributed to the coordinates (x, y, z) corresponding to the desired movement of the reference points of the foot final end.

The objective is to get the two variables of joint θ_2 and θ_3, corresponding to the desired position of the frame final end [5, 6, 7, 11]. In this case, we consider the orientation of the reference frame of the final end, because we are interested in the position. We apply direct kinematic equation (2) and consider the following limitations: all joints are allowed only rotation on an axis, ties have always femur and tibia rotation on parallel axes and limited physical position can be determined for each angle of articulation.

In accordance with the foregoing, the inverse kinematic model of a hexapod robot leg has the following form to joints femur and tibia [1-10]:

$$q_1 = arctan2(x,y) - arctan2\left(l_2 - sin(q_2), l_1 + l_2 cos(q_2)\right) + \frac{\pi}{2}$$
$$q_2 = -arccos\left(\frac{x^2 + y^2 - l_1^2 - l_2^2}{2 l_1 l_2}\right) \quad (6)$$

The inverse kinematics differential link to the desktop speed can be achieved through joint hexapod robot Jacobian matrix, it can be expressed by the following equation:

$$J^{-1}(q) = \begin{bmatrix} h_{11} & h_{12} \\ h_{21} & h_{22} \end{bmatrix}$$
$$h_{11} = \frac{cos(q_1 + q_2)}{l_2 sin(q_1 + q_2) + l_1 sin(q_1) - l_1 sin(q_2)}$$
$$h_{12} = -\frac{sin(q_1 + q_2)}{l_2 sin(q_1 + q_2) + l_1 sin(q_1) - l_1 sin(q_2)} \quad (7)$$
$$h_{21} = -\frac{l_2 cos(2q_1 + 2q_2) + l_1 cos(q_1) + l_1 cos(2q_1 + q_2)}{l_2^2 sin(q_1 + q_2) + l_1 sin(q_1) - l_1 sin(q_2)}$$
$$h_{22} = \frac{l_2 sin(2q_1 + 2q_2) + l_1 sin(q_1) + l_1 sin(2q_1 + q_2)}{l_2^2 sin(q_1 + q_2) + l_1 sin(q_1) - l_1 sin(q_2)}$$

5. Stability and Control of Hexapod Robot

Stability analysis of a robot with multiple legs is necessary to control, especially in dynamic situations on an uneven terrain. The main concept of this type of vehicle stability is that its center of gravity (CG) of the robot must be kept within a stable regions, to prevent its overthrow [7]. Therefore, under both conditions of static and dynamic, when the robot walks, move or handle, it is essential to monitor the stability of the robot at each point using a criterion of stability in the control [11]. In particular while crossing a frame or uneven terrain. There are several criteria for stability of the systems that can be divided into static and dynamic criteria. However, they can be classified on the basis of their stability metric, as follows [1-10]:

Criteria based on distance: distance between each polygon support and projection CG (center of gravity) or the distance between support and force vector polygon net, acting on CG, which is the metric stability. Stability edge (SM), established by McGhee **[5]**, is the most notable distance based on stability, because stability is the edge shown for the first time. MS is defined as the minimum distance between CG and limited support polygonal projection [4, 7, 11].

Angle-based criteria: use the angle of the polygon support and the net force acting on CG accounting system stability. Based on the number of indications of its shares, the most notable criterion in this category is the angular edge stability force (FASMA) **[5]**. FASMA is defined as the net force and angle between the line connecting the center of mass of the rotation point (the plan) and the axis of rotation (in space) [3, 6, 8].

Criteria based on energy: They start from the energy difference between the robot in two different situations and overthrow the current configuration. The first static based on the stability (ESM) was presented by Messuri and Klein in "Automatic body regulation for Maintaining stability of a legged vehicle during rough-terrain locomotion" and the dynamic (DESM) was presented by Ghasempoor and Sepehr in "a measure of stability for moving base machine manipulators", which was normalized by S. Hirose (NESM) and Garcia (NDESM) [1-10]. Most of stability criteria fall under the criteria based on time since overthrowing takes place when the time exceeds one of the axes of rolling. However, the criterion based on time can be quite difficult to implement especially on uneven terrain because it requires understanding of axis and the position of each leg. The most notable moment is the stability criterion based on dynamic image (DSM), zero moment point (ZMP) and Roll Stability edge (TSM) [1-10].

Criterion based on force: the focus is on the forces acting on the robot. When inverting the leg strength, the exception is that the rolling axis or planar point of robot becomes zero. Although attempts have been made to use this concept for controlling the robot, there is no certainty concerning the exact way of monitoring it. Researchers Garcia, Roan and many others have concluded that a mobile robot is controlled by several feet on three levels: the torso, legs and joints [1-11]. This criterion is applied to any mobile robot.

Leg strength - edge stability

In dynamic situations, it is essential to monitor the stability of the robot every time by using a stability criterion, especially while crossing a frame, an undulating ground, as shown in figure 5. According to E. Garcia and P.A.G. Santos, a car in motion is dynamically stable if the time limit j's support polygon is caused by ground forces and moments are positive (in clockwise). It emphasizes that with E. Garcia and P.A.G. Santos used the F × R not R× F. Using R × F, the definition of dynamic stability can be

rewritten as: a running car is stable dynamic if time j which limits the support polygon caused by the ground forces and moment are negative (reverse clockwise). From Newton's law, the following limits must be met in support of the polygon [1-10], each as follows:

$$M_{in,j} = M_{gr,j} + M_{man,j} + M_{sup,j} \quad (8)$$

where $M_{in,j}$ it is the moment due to the inertial force and moment $M_{gr,j}$ it is the moment due to gravity and $M_{man,j}$ it is the moment is due when handling (external) and force and moment $M_{sup,j}$ is the moment based on contact force and moment. All times are calculated on j, support polygon limit. From Equation (8), the following can be written:

$$M_{sup,j} = -\left(M_{gr,j} + M_{man,j} - M_{in,j}\right) \quad (9)$$

The term in brackets from equation (9) is the net moment when acting upon j, the support polygon limit, due to all forces and moments handled. Therefore, it can be replaced with $M_{Net,j}$ which may be offset by moments and ground forces, $M_{sup,j}$.

Therefore, in order to have a stable dynamic of the robot, the following equation must be satisfied:

$$M_{sup,j} = -M_{Net,j} \quad (10)$$

Indicating that a robot to be dynamically stable, the net time support polygons j limit must be positive (in clockwise), but with the same amplitude as support forces and moments due time. Otherwise, the robot will roll. Assuming the point of contact, the legs point, the equation can be written accounting $M_{sup,j}$:

$$M_{sup,j} = \sum_{i=1}^{n} R_i \times F_i = \sum_{i=1}^{n} f_i \cdot R \times \left(\sqrt{1+\mu_i^2} \cdot e_{F,i}\right) \quad (11)$$

where n is the number of the legs, R_i is the position vector perpendicular to the contact of the feet, on the limit j support, F_i foot is in contact force vector, $f_i = \|f_i\|$ amplitude is the normal leg strength, where f_i it is a normal component of F_i shown in figure 6. μ_i is the friction of the foot / ground and $e_{F,i}$ is the unit vector of force foot contact, F_i.

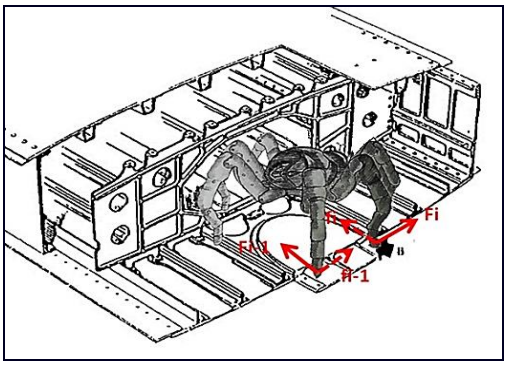

Figure 6: The robot studied in the fuel tank (robot has n foots and is on an uneven terrain)

Therefore, the dynamic stability of normal strength correlates with the robot foot (f_i), as well as the coefficient of friction (μ_i) and foot positions (R_i) in accordance with E. Garcia and P.A.G. Santos in the paper "A new energy dynamic stability margin for walking machines", in International Conference on Advanced Robotics, pp. 1014-1019, 2003 equations (10) and (11). However, to analyze the stability of an ideal robot with multiple legs, the friction coefficient is considered high enough to prevent slippage of the robot. Therefore, the instability is considered overturning / rolling not slipping. It is assumed that the distribution leg is necoliniar, $\sum_{i=1}^{n} \|R_i\| \neq 0$. Also, all contacts between the legs of the contact surfaces are assumed to be contact point [1-10].

Giving the robot with multiple legs (n≥3) with only two forces strictly positive, indicating that only two legs are in contact with the ground, creating j limited support, it is determined that $M_{sup,j}$ is zero and requires $M_{Net,j}$ to be the same, namely zero. Otherwise, if $M_{Net,j} \neq 0$, equation 10 will be satisfied and the robot will roll. Therefore, to be considered dynamic stability, the robot must have at least one foot on the ground with a force strictly positive to negative because of a time limit on support and to offset the positive j, $M_{Net,j}$. If $M_{Net,j}$ is negative, the robot is unstable [2-7].

Taking into account the assumptions in the above discussion, it is assumed the following conclusion:

Definition 1 - ideal mobile robot with n foot (n≥3) at time *t* is dynamically stable if and only if there are at least three non-collinear legs and a strictly positive force $(f_i > 0)$ at time *t* [11]. This definition provides a quick method for determining

measurable system stability. However, it neglects R_i, which greatly influences $M_{sup,j}$ [2, 4, 7].

The current relationship between stability and leg strength requires strictly positive forces $(f_i > 0)$; however, the relationship may change if considering riding on walls, frames, ceilings and surfaces very inclined [3, 5, 8].

As shown in the above finding, the stability occurs when there are at least three feet forces of the leg strictly positive. Intuitively, stability occurs when the maximum size of the leg forces are all the same, that forces of the legs are all the same and the forces are evenly distributed on all four feet. It is desirable to have an appropriate understanding that provides a normalized current stability of the system based on force amplitude leg. FFSM uses forces of foot and foot stability to describe their status [4, 7, 10].

It allows $f_1, f_2, \ldots, f_n$ amplitude to be normal force to support legs. The product of all forces leg, $\prod_{i=1}^{n} f_i$ is used as a basis to define FFSM since it satisfied the definition of 1 instability. FFSM maximum stability of the robot, the product is normalized between 0 and 1. For this purpose, the ratio of force - the total force measured individual leg, $\frac{f_i}{f_{tot}}$, it is used when $f_{tot} = \sum_{i=1}^{n} f_i$ is observed that $\sum_{i=1}^{n} \frac{f_i}{f_{tot}} = 1$.The maximum amplitude $\prod_{i=1}^{n} \frac{f_i}{f_{tot}}$ is $\frac{1}{n^n}$ which correlates with the condition of maximum stability of the machine. For FFSM to result in a number between 0 to state 1 state unstable and stable maximum term n^n it is multiplied by the product. FFSM at time t for a robot with n foot support is defined as:

$$FFSM = S = \prod_{i=1}^{n} \frac{f_i}{\bar{f}}, \quad 0 \le S \le 1 \tag{12}$$

where n is the number of the legs with strictly positive forces on foot and $\bar{f} = \frac{f_{tot}}{n}$ there is the average of all normal forces on foot. Therefore, FFSM is based on the fractions to the average of all the forces of the foot [4, 8, 10]. Equation (12) provides an amplitude stability margin between zero and one, 0≤S≤1, indicating how close the system is to achieve maximum state of instability or stability condition. As expected, the equation (12) shows that a uniform distribution of forces improves the stability of the whole system legs. Therefore, maximum stability FFSM = 1, occurs only when the forces are evenly distributed on foot, that is to say the standard deviation of the amplitude of the force of the foot is zero [1-10].

Given a system n≥4 and m standing m≤n-3, due to the loss of contact with the ground, which usually happens on an uneven terrain. Stability will indicate a zero edge while the system will remain stable with n - m support legs. For example, when a robot walks, configuration changes from quadruped, n = 4 from the tripod, n = 3, a foot loses contact with the ground while the tripod support configuration maintains stability. In order to take into account, the loss of contact with the ground on purpose, in the calculating FFSM should be updated accordingly to n← n – m at each iteration in the controller. To ensure that the robot will be stable after switching from n to n -m feet FFSM both states must be calculated simultaneously while the robot switches. Thus, if n -m is not a stable configuration, the robot will recognize and will not fall [1-10].

Since the FFSM only focuses on the amplitude of the normal component of the forces of the foot, taking into account the cross-section of the leg of the robot, on the assumption that α > 1 is a constant, FFSM is the same for all four cases:

$$MFFSM = m\,(t)\,S \tag{13}$$

6. Modeling and Simulating the Movement of the Hexapod Mobile Robot Using Labview 14.0

Using the LabView 14.0 program, were analyzed the parameters of speed, angular displacement and final position of the legs and these are shown in the images below figs. 7-15.

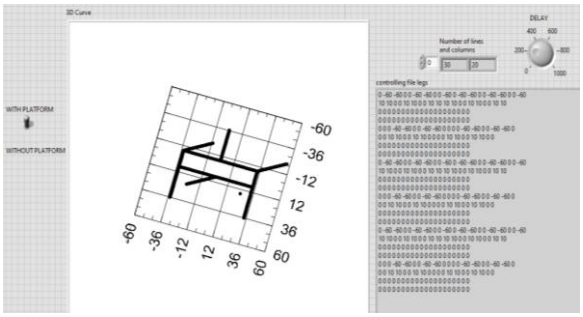

Figure 7: Front panel of movement simulation in 3D hexapod schema of robot and file command of the S2, D1 and D3 legs

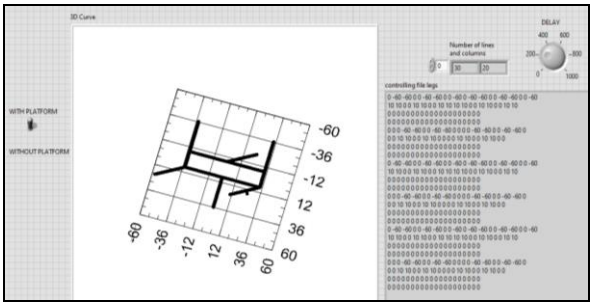

Figure 8: Movement of the S1, S3 and D2 hexapod mobile robot's legs

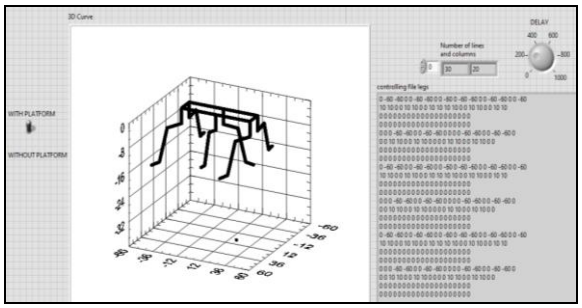

Figure 9: 3D movement of the hexapod mobile robot's legs

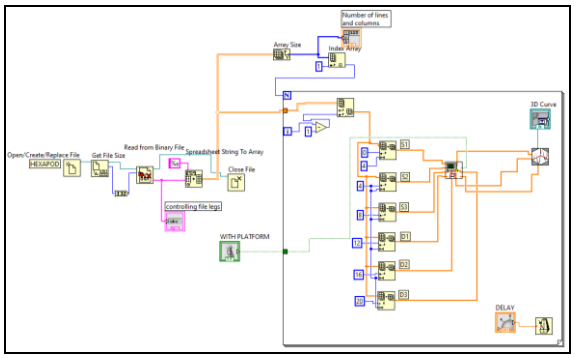

Figure 10: LabView Bloc Diagram of the hexapod mobile robot

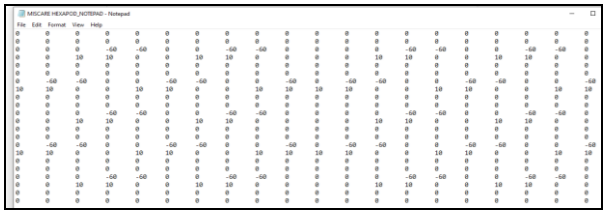

Figure 11: Command file with numerical parameters of the hexapod mobile robot

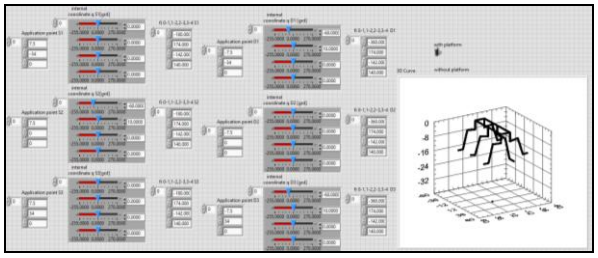

Figure 12. Front panel of the SubVI-s LabVIEW of the hexapod mobile robot with control blocks of each robot's leg

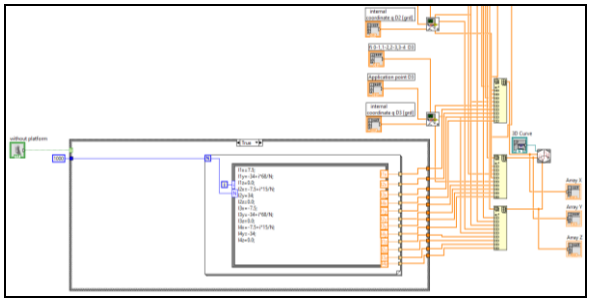

Figure 13. Part of the LabView Bloc Diagram of the remote control of hexapod mobile robot

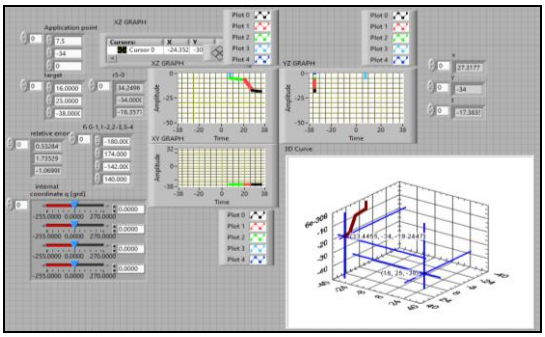

Figure 14: Front panel for simulation of one leg robot

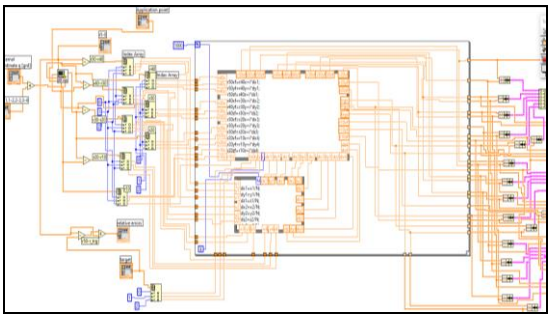

Figure 15: LabView Bloc Diagram of the hexapod mobile robot

The simulation movements of the hexapod robot content some *SubVI*-s designed for the legs, the mobile platform and the hexapod, figs.3-5. Fig.6 content the LabVIEW block diagram for simulating the movement of the hexapod in the variant of movement: three legs with simultaneous movement leg S1, S3 (left legs) and D2 (right leg) and three legs remaining on the ground, legs that ensure the flatness of the hexapod. The file of animation this type of movement is shown in fig.7. Hexapod robot is one multi-robot application that consist in one platform and 6 legs robots, fig.8 each of them with different base application point. These legs could be moved separately and the home position of each of them could be established also separately. LabVIEW block diagram of the remote control of hexapod robot is shown in fig.9. The *SubVI*-s of one robot leg, figs.10-11 have some control modules for each internal home coordinates and variable coordinates with the possibilities of the remote control of each of the joints. This *SubVI*-s assure very easily solving the Forward Kinematics (FK) and Inverse Kinematics (IK) of this type of robot (leg robot). In his block diagram structure, there is one module for FK to show, for each command, the new position of each joint and animation of these.

7. Aircraft Fuel Tank Inspection with the Hexapod Mobile Robot

The practical application was carried out in a hangar, on a Boeing 737-300 aircraft (fig. 16), and the aircraft was in type C control [13]. This type of control is carried out only inside a hangar, and

during this verification, most aircraft systems and subsystems are dismantled for detailed inspection and verification, then reassembled and tested for safety and continuing airworthiness certification [13]. I must point out that not all type C controls also include the inspection of the inside of the aircraft's fuel tank [13]. Regarding the Boeing 737-300 aircraft on which I performed the experiment I found that:

→ the tank has been inspected following a previous work;

→ controls and monitoring of the tank were performed, consisting in the exclusion of some old rivets and the installation of new ones.

This work was done to prevent fuel leakage.

Figure 16: Boeing 737-300 aircraft on which the practical application was made [14]

To make the practical application of the aircraft fuel tank inspection, we used a hexapod mobile robot and went through the following steps:

Step 1: Carefully study the documents and understand the inspection inside the aircraft's fuel tank. These are also called work tasks [13].

The mobile robot would be the solution to reduce the time that technical staff spends inside the tank, which, as mentioned above, is an extremely toxic environment.

Step 2: Access to the tank [13]. In order to reach the central fuel tank of the airplane where the inspection is to be performed, several pipes and the whole of the air conditioning part of the airplane cabin are dismantled, as can be seen in figure 17.

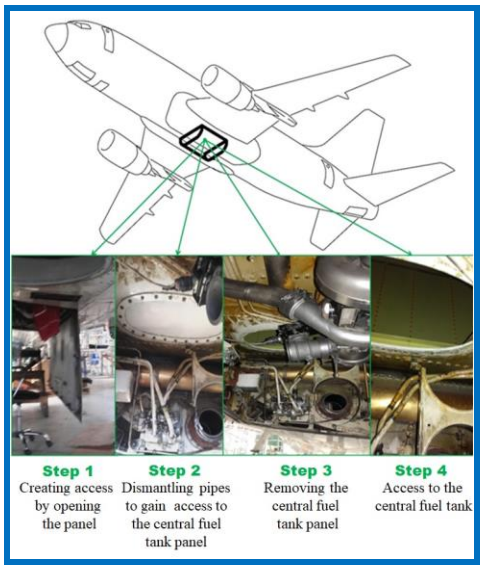

Figure 17: Access to the fuel tank of the Boeing 737-300 aircraft

Step 3: Venting the tank [13]. The ventilation is very important, because the environment is very toxic and the kerosene vapors are very strong. Ventilation can take between 7 days and 2 weeks to reduce as much as possible the amount of kerosene vapor and other gases.

After the ventilation period ended, I started the actual practical application. As can be seen in the figure below (fig. 18), the access is quite difficult to achieve, because the entrance area to the tank is quite limited.

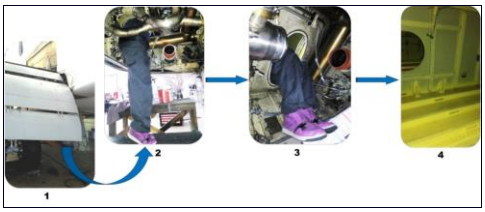

Figure 18: Entrance to the central fuel tank of the Boeing 737-300 aircraft

Figure 19: Removal of traces of kerosene left in the central fuel tank of the Boeing 737-300 aircraft

Step 4: The actual inspection performed by the robot. The shape of the tank is massive, consisting of frames of up to 7 mm, as can be seen in fig. 20.

That was why I used a hexapod robot with elongated legs. Thus, the robot can go over the frames, only with a slight difficulty, depending very much on the operator's coordination.

But once inside the tank, the robot was able to perform the inspection, as shown in the figures below.

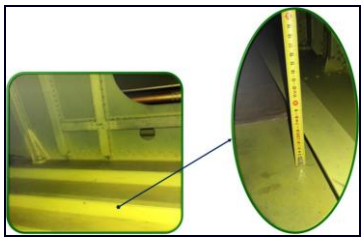

Figure 20: Identification and measurement of frames in the central fuel tank of the Boeing 737-300 aircraft

It is very important to mention that, by identifying the frames and measuring them (see fig. 20) we were able to establish the limits of the hexapod mobile robot.

The measured frames are 7 mm and as a result, we designed the length of the robot's legs, in order to

overcome the obstacles in the tank, as can be seen in Fig. 21.

The hexapod mobile robot was guided by a smartphone, but I must point out that the operation and guidance of the operator is the main basis in overcoming all obstacles, so that the hexapod mobile robot can complete the task of inspecting the tank aircraft fuel plant.

I made the practical application in two ways. In the first method, the operation and guidance of the hexapod mobile robot was performed inside the central fuel tank of the aircraft, and in the second method, from outside it. By the first method, I set out to observe the movement of the robot inside the tank.

We watched very carefully if the robot could overtake the frames and if it could move, even when there were still traces of kerosene in the tank.

The experiment was successfully completed, and the hexapod mobile robot overcame all obstacles, as can be seen in the figure below.

Figure 21: The hexapod mobile robot inside the central fuel tank of the Boeing 737-300 aircraft

The **second method** was to guide the hexapod mobile robot from outside the tank, which was a challenge. The question has been whether the travel commands will reach the robot in real time. It was only equipped with a Sony camcorder [22], and the commands were transmitted from a smartphone.The images transmitted by the Sony video camera [22] were practically the ones I saw on the phone and in this way, I gave commands, through which the robot began to move slowly. I must point out that I performed the experiment very close to the plane, at a relatively short distance from the robot, more precisely, close to the entrance to the central fuel tank of the plane.

At the beginning, with great caution, I managed to give the robot a command for slow movement. The average speed of the robot was 3 m / min. The Sony camcorder gave me a real advantage, because the image quality was impeccable and this can be seen in the images presented. Every moment of the experiment was captured by the video camera, but I focused on the inspection of the tank. A very important thing must be emphasized, namely the fact that we achieved efficient communication between the phone we used and the hexapod mobile robot.

When I moved about 3 meters away from the plane, I found that the signal remained just as good and in this way, I assumed that the guidance / control of the robot can be done from a greater distance.

The inspection of the central fuel tank of the aircraft with the help of the hexapod mobile robot was carried out and completed successfully, because: the robot-human communication was very good; the robot moved in the tank with a speed of 3 m / min, being able to capture the frames that I wanted to highlight in particular and that followed the installation of rivets. The time in which the inspection of an area of 5 meters took place was 15 minutes in which 10 images were taken.

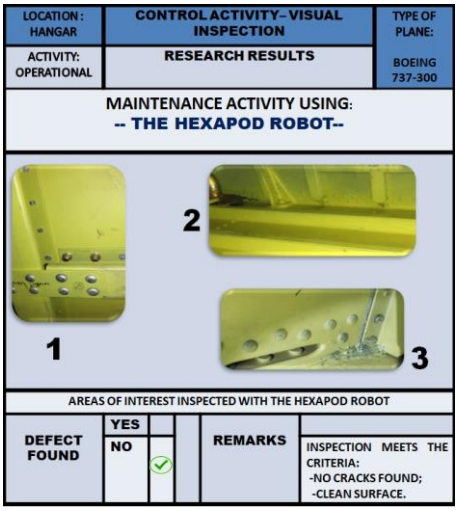

Figure 22: Images transmitted by the hexapod mobile robot

The images transmitted by the robot (fig. 22) showed that the tank complies with the AMM (Aircraft Maintenance Manual) [13] norms, the rivets are mounted properly and we did not notice any malfunction leading to a possible fuel leak on the aircraft fuselage.

8. Conclusions

Following this analysis of work in the aircraft's fuel tank, it appears that this working environment is very harmful to humans. Therefore, the main purpose of this paper is to solve this problem by introducing a mobile robot. This robot should not be seen as an obstacle in developing the capabilities of the human factor, but helping it..

Following the experiment, we came to the conclusion that the hexapod mobile robot managed to meet all the requirements imposed by the inspection procedures. The inspection took place over a period of 2 hours, and the average speed of the robot was 3 m / min, given that the geometry of the robot's configuration allows the correct movement inside the tank.

Following the practical application, we demonstrated that the maintenance can be improved by integrating a robot, which would bring great benefits to the human operator, because the aircraft's fuel tank is an extremely harmful environment, which can affect human physical and mental health, while the robot can successfully intervene and help.

Through the LabView program, the parameters of the robot's legs could be determined, taking into account a minimum margin of error. It was also possible to observe the possibilities of movement of the robot so that it is properly adapted for work inside of the aircraft fuel tank.

References

[1] A. Ghasempoor and N. Sepehri, *A measure of machine stability for moving base manipulators*, in Proceedings of the IEEE International Conference on Robotics and Automation, vol. **3**, pp. 2249, 2254, 1995.

[2] S. Hirose, H. Tsukagoshi and K. Yoneda, *Normalized energy stability margin: Generalized stability criterion for walking vehicles*, in Proceedings of International Conference on Climbing and Walking Robots, pp. 71,76, 1998.

[3] E. Garcia and P. A. G. de Santos, *A new dynamic energy stability margin for walking machines*, in Proceedings of International Conference on Advanced Robotics, pp. 1014,1019, 2003.

[4] J. K. Davidson and G. Schweitzer, A mechanics-based computer algorithm for displaying the margin of static stability in four-legged vehicles, *Transaction of the ASME Journal of Mechanical Design*, vol. **112**, no. 3, pp. 480,487, 1990.

[5] B.-S. Lin and S.-M. Song, *Dynamic modeling, stability and energy e_ciency of a quadrupedal walking machine*, in Proceedings of the IEEE International Conference on Robotics and Automation, vol. **3**, pp. 367,373, 1993.

[6] S. Sugano, Q. Huang and I. Kato, *Stability criteria in controlling mobile robotic systems*, in Proceedings of the IEEE/RSJ International Conference on Intelligent Robots and Systems, vol. **2**, pp. 832,838, 1993.

[7] D.-O. Kang, Y.-J. Lee, S.-H. Lee, Y. S. Hong and Z. Bien, *A study on an adaptive gait for a quadruped walking robot under external forces*, in Proceedings of the IEEE International Conference on Robotics and Automation, vol. **4**, pp. 2777,2782, 1997.

[8] Q. Huang, K. Tanie and S. Sugano, Coordinated motion planning for a mobile manipulator considering stability and manipulation, *The International Journal of Robotics Research*, Vol **19**, issue 8, page(s): 732-742, https://doi.org/10.1177/02783640022067139, Issue published: August 1, 2000.

[9] J. Kim, W. K. Chung, Y. Youm and B. Lee, *Real-time zmp compensation method using null motion for mobile manipulators*, in Proceedings of the IEEE International Conference on Robotics and Automation, vol. **2**, pp. 1967 , 1972, 2002.

[10] J.-H. Lee, J.-B. Park and B.-H. Lee, Turnover prevention of a mobile robot on uneven terrain using the concept of stability space, *Robotica*, vol. **27**, no. 05, pp. 641,652, 2009.

[11] K. Yoneda and S. Hirose, *Tumble stability criterion of integrated locomotion and manipulation*, in Proceedings of the IEEE/RSJ International Conference on Intelligent Robots and Systems, vol. **2**, pp. 870,876, 1996.

[12] *** http:/www.image-sensing-solutions.eu

[13] AMM (*Aircraft Maintenance Manual*).

[14] *** http://www.boeing.com

[15]***http://www.boeing.com/commercial/aeromagazine/aero_04/textonly/s01txt.htm

[16]*** http://www.epa.gov/hpv/pubs/summaries/kerjetfc/ c15020ad2.pdf

[17]*** http://www.conidia.com/downloads/md8_info_sheets_spanish/Hoja_informativa_marina_1.pdf [18]*** https://www.faa.gov/regulations.../aircraft/amt.../ ama_ch14.pdf

[19] ASTM D6469 – 14, Para 8.3 – 8.6, Standard Guide for Microbial Contamination in Fuels and Fuel Systems

[20] IATA (International Air Transport Association) Guidance Material on Microbial Contamination in Aviation Fuel Tanks. (link: International Air Transport Association)

[21]*** http://www.echamicrobiology.com

[22] *** www.image-sensing-solutions.eu

[23]***https://conidia.com/fuel-testing-kits/fuelstat-plus/